

Evaluating Power System Vulnerability to False Data Injection Attacks via Scalable Optimization

Zhigang Chu, Jiazi Zhang, Oliver Kosut, and Lalitha Sankar
School of Electrical, Computer, and Energy Engineering
Arizona State University
Tempe, AZ, 85287

Abstract—Physical consequences to power systems of false data injection cyber-attacks are considered. Prior work has shown that the worst-case consequences of such an attack can be determined using a bi-level optimization problem, wherein an attack is chosen to maximize the physical power flow on a target line subsequent to re-dispatch. This problem can be solved as a mixed-integer linear program, but it is difficult to scale to large systems due to numerical challenges. Three new computationally efficient algorithms to solve this problem are presented. These algorithms provide lower and upper bounds on the system vulnerability measured as the maximum power flow subsequent to an attack. Using these techniques, vulnerability assessments are conducted for IEEE 118-bus system and Polish system with 2383 buses.

I. INTRODUCTION

With integration of real-time monitoring, sensing, communication and data processing, electric power systems are becoming increasingly efficient and intelligent. However, similar to all computer network integrated systems, this integration also makes power systems more vulnerable to cyber attacks which could result in serious physical consequences or even system failure. Therefore, it is crucial to evaluate system vulnerability to credible attacks before they happen, and develop techniques to detect potential attacks and protect the system.

False data injection (FDI) involves a malicious adversary replacing a subset of measurements with counterfeits. It has been shown that FDI attacks can be designed to target system states [1], [2], [3], system topology [4], [5], generator dynamics [6], and energy markets [7]. Some of these involve designing an optimization problem to determine the worst-case FDI attacks that can cause line overflow [8], operating cost change [9], [10], or locational marginal price change [11]. However, the results are only demonstrated for small systems. Similar to [8], we consider an optimization problem to determine the worst-case FDI attack that causes line overflow, but our goal is to design optimization algorithms that scale to significantly larger systems (*i.e.* thousands of buses).

In [8], an FDI attack against state estimation (SE) that leads to an overflow is introduced. Subsequent to the attack, the system operator re-dispatches the system generation, leading to an overload on a target line. Modeling such attacks leads to formulation of a bi-level optimization problem in which the first level models the attacker's ability and limitations while the second level models the system response via optimal power flow (OPF). This bi-level optimization problem is reformulated to a single level mixed-integer linear problem

(MILP) by replacing the second level by its Karush-Kuhn-Tucker (KKT) conditions and rewriting the non-convex complementary slackness conditions as mixed integer constraints.

As the system size scales, this optimization problem becomes hard to solve because of the increasing number of constraints as well as number of binary variables. But the recent cyber attack in Ukraine (see [12]) reminds us that it is imperative to characterize the vulnerability of large power systems. To this end, we introduce three computationally efficient algorithms to characterize the vulnerability of systems. In some cases, these algorithms give the optimal attack. In other cases, finding the optimal attack is intractable, so instead these algorithms provide lower and upper bounds on the optimal objective value. A lower bound represents a feasible solution, and thus, highlights a specific overflow vulnerability for the system. An upper bound, on the other hand, constitutes a limit on the severity of this class of attacks.

The first algorithm provides the optimal solution to the problem by reducing the number of line thermal limit constraints as well as the binary variables associated with them. The second algorithm further reduces the number of generation limit constraints and corresponding binary variables. However, by doing this we give up a guarantee on optimality, so the algorithm only provides a lower bound on the objective. The third algorithm provides both a lower bound and an upper bound via linear programming (LP) that maximizes the difference between target line cyber and physical power flows. All three algorithms are tested on the IEEE 118-bus system and the Polish system (2383 buses) to evaluate system vulnerability.

The outline of this paper is as follows. In Sec. II, power system state estimation and the attack model are described. Sec. III describes how to formulate the bi-level optimization problem and how to convert it to a MILP, while Sec. IV introduces three algorithms to solve such optimization problem. Simulation results and concluding remarks are presented in Sec. V and VI, respectively.

II. STATE ESTIMATION AND ATTACK MODEL

In this section, we introduce the mathematical formulation for SE and the attack model. Throughout, we assume there are n_b buses, n_{br} branches, n_g generators, and n_m measurements in the system. For tractability, we focus on the DC power flow

model and DC SE, but the attacks introduced in this paper can also be performed against AC SE as in [8].

A. State Estimation

The DC measurement model is described as

$$z = Hx + e \quad (1)$$

where z is the $n_m \times 1$ measurement vector whose entries are measurements of the system; x is the vector of bus voltage angles; H denotes the $n_m \times n_b$ matrix describing the relationship between the system states and measurements; e is the $n_m \times 1$ measurement error vector, whose entries are assumed to be independent and Gaussian distributed with zero mean and covariance matrix $R = \text{diag}(\sigma_1^2, \sigma_2^2, \dots, \sigma_{n_m}^2)$.

Observability analysis is performed before the state estimation process to check whether the system is fully observable. The weighted least-square (WLS) method is utilized to solve the SE problem, and the solution is given by [1]

$$\hat{x} = (H^T R^{-1} H)^{-1} H^T R^{-1} z \quad (2)$$

where \hat{x} is the estimated system state vector. We assume classical bad data detection, based on measurement residuals, is used to detect large errors in measurement data. Note that traditional bad data detectors cannot necessarily detect FDI attacks. Indeed, unobservable attacks, as defined below, cannot be detected by any bad data detector based on measurement residuals.

B. Attack Model

We first assume that the attacker has the following knowledge and capabilities:

- 1) The attacker has full system topology information via power transfer distribution factors (PTDF).
- 2) The attacker has knowledge of load distribution, generation costs and line thermal limits of the system.
- 3) The attacker has control of the measurements in a subset \mathcal{S} of the network.

As discussed in [8], in the absence of noise, an attack is defined to be *unobservable* when there exists an $n_b \times 1$ attack vector $c \neq 0$ such that for all i , the measurement \bar{z}_i modified by the attacker satisfies $\bar{z}_i = z_i + H_i c$, where H_i denotes the i^{th} row of H . Given an attacker with control of the measurements in \mathcal{S} , it can execute this attack with attack vector c if $H_i c$ has non-zero entries only in \mathcal{S} .

Given an attack vector c , the following procedure produces a subgraph \mathcal{S} that, if controlled by the attacker, can execute an unobservable attack. For an attack vector c , *load buses* (i.e., buses with load) corresponding to non-zero entries of c are denoted as *center buses*. Given an attacker vector c , the subgraph \mathcal{S} controlled by the adversary is constructed using the following algorithm introduced in [3]:

- 1) Let \mathcal{S} be the set of all center buses.
- 2) Extend \mathcal{S} by including all branches and buses adjacent to center buses.

- 3) If any bus on the boundary of \mathcal{S} is a *non-load bus* (i.e., no load is present), extend \mathcal{S} by including all adjacent branches and buses to this bus.
- 4) Repeat step 3) until all boundary buses are load buses.

Constructing \mathcal{S} with this method ensures that only measurements inside \mathcal{S} can be modified by the attacker. The system operator will see the results of this unobservable attack as load changes at load buses within \mathcal{S} , while the total load of the system remain unchanged.

III. WORST-CASE LINE OVERFLOW ATTACKS

In [8], a bi-level optimization problem is introduced to find the worst-case unobservable line overflow attack vector given the attacker's limited resources to change states. In the optimization problem, the first level models the attacker's objective to maximize the power flow on a target line, subject to constraints on (1) the attacker's resources, characterized by the number of center buses in c , and (2) the attacker's detectability, characterized by the load shift, or the difference between the cyber load and the original load, as a percentage of the original load. The second level is a DCOPF problem simulating the system response to the attack. It is demonstrated in [8] that unobservable attacks solved with the MILP can successfully lead to generation re-dispatch that maximize physical power flow on the target line, and hence, can result in line overflow for IEEE RTS 24-bus system.

In [8], B - θ method is used to formulate the DCOPF problem, where the line power flow is calculated as the product of the dependency matrix of power flow and voltage angle B and the voltage angle vector θ . In contrast, in this paper we equivalently formulate the DCOPF using PTDF, where the line power flow is calculated as the product of PTDF matrix and power injection. Note that in this formulation, the variable vector θ is eliminated, and hence, the thermal limit constraints become independent of each other. Without loss of generality, we assume the power flow on the target line is positive. If it is not, we just maximize the negative of it.

The bi-level optimization problem is formulated as follows: (dual variables for second level problem are written in parentheses)

$$\underset{c}{\text{maximize}} \quad P_l - \sigma \|c\|_1 \quad (3)$$

subject to

$$P = \text{PTDF}(G_B P_G^* - P_D) \quad (4)$$

$$\|c\|_1 \leq N_1 \quad (5)$$

$$-L_S P_D \leq Hc \leq L_S P_D \quad (6)$$

$$\{P_G^*\} = \arg \left\{ \min_{P_G} C_G(P_G) \right\} \quad (7)$$

subject to

$$\sum_{g=1}^{n_g} P_{Gg} = \sum_{i=1}^{n_b} P_{Di} \quad (\lambda) \quad (8)$$

$$-P^{\max} \leq \text{PTDF}(G_B P_G - P_D + Hc) \leq P^{\max} \quad (F^\pm) \quad (9)$$

$$P_G^{\min} \leq P_G \leq P_G^{\max} \quad (\alpha^\pm) \quad (10)$$

where the variables:

c is the $n_b \times 1$ attack vector;
 P is the $n_{br} \times 1$ vector of physical line power flow;
 P_l is the physical power flow of target line l ;
 P_G, P_G^* are $n_g \times 1$ vectors of generation dispatch variables and optimal generation dispatch solved by DCOPTF, respectively;
 λ is the dual variable of the generation-load balance constraint;
 F^+, F^- are $n_{br} \times 1$ dual variable vectors of the upper and lower bound of thermal limits, respectively;
 α^+, α^- are $n_g \times 1$ dual variable vectors of the upper and lower bound of generator capacity limits, respectively;

and the parameters:

L_S is the load shift factor;
 P_D is the $n_b \times 1$ vector of active load at each bus;
 N_0 is the l_0 -norm constraint integer;
 H is the $n_b \times n_b$ dependency matrix between power injection measurements and state variables;
 G_B is the $n_b \times n_g$ generator to bus connectivity matrix;
 C_G is the cost function of the generation vector;
 P^{\max} is the $n_{br} \times 1$ vector of line thermal limit;
 P_G^{\min}, P_G^{\max} are $n_g \times 1$ vectors of minimum and maximum generator output, respectively;
 σ is the weight of the norm of attack vector c .

In the first level objective function, σ is chosen to be a small positive number to minimize the contribution of the second term in the objective; constraint (4) calculates the physical power flow of the system; constraint (5) models the limited resources that the attacker can use to change states. Ideally, the l_0 -norm would be used, giving the exact sparsity of c , but for tractability we use the l_1 -norm as a proxy. Constraint (6) ensures the load changes are small enough to avoid detection. In the second level, the system response to the attack vector determined in the first level is modeled via DCOPTF as in (7)–(10).

The bi-level optimization problem introduced above is non-linear. We modify several constraints to convert the original formulation into an equivalent MILP as in [8]. The modifications include:

- 1) Linearize the l_1 -norm constraint in (5) by introducing a slack vector s as

$$c \leq s, \quad -c \leq -s, \quad \sum_{i \in \mathcal{L}_{\text{load}}} s_i \leq N_1 \quad (11)$$

where $\mathcal{L}_{\text{load}}$ is the set of load buses. Meanwhile, the objective function (3) becomes

$$\underset{c, s}{\text{maximize}} \quad P_l - \sigma \sum_{i \in \mathcal{L}_{\text{load}}} s_i \quad (12)$$

- 2) Replace the second level DCOPTF problem by its KKT optimality conditions as introduced in [13], as

$$(8) - (10)$$

$$\begin{aligned} \mathbf{0} = & \nabla [C_G(P_G)] + \nabla \left(\sum_{g=1}^{n_g} P_{Gg} - \sum_{i=1}^{n_b} P_{Di} \right) \cdot \lambda \\ & + \nabla [\text{PTDF}(G_B P_G - P_D + Hc) \mp P^{\max}] \cdot F^\pm \\ & + \nabla (P_G - P_G^{\max}) \cdot \alpha^+ + \nabla (P_G^{\min} - P_G) \cdot \alpha^- \end{aligned} \quad (13)$$

$$\mathbf{0} \leq F^\pm \quad (14)$$

$$\mathbf{0} \leq \alpha^\pm \quad (15)$$

$$\mathbf{0} = \text{diag}(F^\pm) [\text{PTDF}(G_B P_G - P_D + Hc) \mp P^{\max}] \quad (16)$$

$$\mathbf{0} = \text{diag}(\alpha^+) (P_G - P_G^{\max}) \quad (17)$$

$$\mathbf{0} = \text{diag}(\alpha^{-T}) (P_G^{\min} - P_G) \quad (18)$$

where constraint (13) is the partial gradient optimal condition, (14) and (15) are the dual feasibility constraints, (16)–(18) represent the complementary slackness constraints.

- 3) Linearize the complementary slackness constraints in KKT conditions by introducing new binary variables δ and a large constant M as

$$[\delta_F^\pm; \delta_\alpha^\pm] \in \{0, 1\} \quad (19)$$

$$\begin{cases} F^\pm \leq M \delta_F^\pm \\ P^{\max} \mp \text{PTDF}(G_B P_G - P_D + Hc) \leq M(1 - \delta_F^\pm) \end{cases} \quad (20)$$

$$\begin{cases} \alpha^\pm \leq M \delta_\alpha^\pm \\ P_G^{\max} - P_G \leq M(1 - \delta_\alpha^+) \\ P_G - P_G^{\min} \leq M(\delta_\alpha^- - 1) \end{cases} \quad (21)$$

The whole problem then becomes a single level MILP with objective (12), subject to (4), (6), (8)–(11), (13)–(15), and (19)–(21). Throughout this paper, this problem is denoted as *the original MILP* with P_l^* as the optimal objective. This problem is NP-hard, thus it is not guaranteed that a solution can be found in polynomial time. As the system network size scales, the number of binary variables increases, resulting in an increased computational burden. We have found experimentally that for the IEEE 118-bus system, the original MILP fails to converge in a reasonable length of time using solver GUROBI. Since power systems in the real world are typically very large (*e.g.*, the PJM system includes 15000 buses, 2800 generators and 20000 branches), a straightforward approach to solving this problem for real-world systems does not allow a characterization of the worst-case attacks.

IV. COMPUTATIONAL EFFICIENT ALGORITHMS TO SOLVE ATTACK OPTIMIZATION PROBLEMS

In this section, we introduce three computational efficient algorithms to overcome the computational challenges brought on by a large number of binary variables. Algorithm 1 (A1) reduces the number of line thermal limit constraints as well as the number of binary variables associated with them from the original MILP. If it converges, the optimal objective $P_l^{*(A1)}$ solved with Algorithm 1 is guaranteed to be equal to the

optimal objective of the original MILP. However, as the system size scales, even though the number of binary variables associated with line thermal limit constraints is significantly reduced, the number of binary variables associated with generation limit constraints is still large enough to make the problem hard to solve. As an experimental verification, we note that Algorithm 1 works efficiently for the IEEE 118-bus system, but it fails to converge in a reasonable length of time for the Polish system with 2383 buses. Thus, similar to Algorithm 1, we propose Algorithm 2 (A2), in which we further reduce the number of generation limit constraints as well as the binary variables associated with them from the original MILP. Algorithm 2 gives a feasible solution, but the solution can be sub-optimal. Thus, the resulting objective value $P_l^{*(A2)}$ is a lower bound on P_l^* . Finally, we propose Algorithm 3, which maximizes the difference between the target line cyber and physical power flows, to evaluate system vulnerability without modeling the system response to the attack. This reduces to a linear program, whose optimal solution can be used to derive both a lower bound $P_l^{*(A3,lb)}$ and an upper bound $P_l^{*(A3,ub)}$ on P_l^* . A comparison of these three algorithms is given in Table I.

A. Reducing the Number of Binary Variables Associated with Line Thermal Limit Constraints

In [14] and [15], the authors suggest that a constraint reduction technique can be used to accelerate the solving process for optimization problems for large power systems, such as unit commitment and security constrained economic dispatch (SCED). The thermal limit constraints which are likely to be non-binding at the optimal solution are removed for speed. In Algorithm 1, we apply a similar method to improve the efficiency of the original MILP by reducing the number of binary variables associated with line thermal limits constraints. For lines whose pre-attack power flow are much lower than their ratings, their thermal limit constraints are unlikely to be binding in the optimal solution of the optimization problem, and hence, can be removed. Thus, we propose Algorithm 1 to remove constraints from (19) and (20) without violating any constraints of the original MILP.

Algorithm 1 Attack optimization problem with reduced thermal limit constraints

- 1) Perform a system wide DCOPF assuming no attack is present.
 - 2) Let \mathcal{Q} be the set of lines whose power flow are more than 90% of ratings (denote as *critical lines*).
 - 3) For each line k , if $k \notin \mathcal{Q}$, remove the corresponding constraints from (9), (13)–(14), (19), and (20).
 - 4) Solve the reduced problem, and use the optimal dispatch $P_G^{*(A1)}$ to calculate the cyber power flow of the system.
 - 5) If there exists any cyber overflow, add those lines to \mathcal{Q} , and go back to 3).
 - 6) Let $P_l^{*(A1)}$ be the optimal objective value of the reduced problem.
-

If the algorithm terminates, the solution is guaranteed to be

the optimal solution of the original MILP (i.e. $P_l^{*(A1)} = P_l^*$) because no thermal limits are violated.

B. Reducing the Number of Binary Variables Associated with Power Generation Limit Constraints

Algorithm 2 modifies Algorithm 1 by further reducing the number of binary variables, now focusing on generation limit constraints. Since constraint (6) ensures the load changes are small, the generation re-dispatch is likely to be limited within a small number of generators (denote as *marginal generators*) corresponding to these load changes. Algorithm 2 reduces the number of binary variables associated with generators by assuming the generation level of non-marginal generators remains unchanged after attack.

Algorithm 2 Attack optimization problem with reduced thermal limit & generation limit constraints

- 1) Perform a system wide DCOPF assuming no attack is present.
 - 2) Let \mathcal{Q} be the set of critical lines as defined above.
 - 3) Let \mathcal{R} be the set of marginal generators. i.e., the set of generators g where $P_{Gg}^{\min} < P_{Gg} < P_{Gg}^{\max}$.
 - 4) For each line k and each generator g , if $k \notin \mathcal{Q}$ and $g \notin \mathcal{R}$, remove the corresponding constraints from (9)–(10), (13)–(15) and (19)–(21).
 - 5) Solve the reduced problem, then take the optimal attack vector c_{A2}^* to run post-attack DCOPF (7)–(10) to get system operator's corresponding dispatch P_G^{post} .
 - 6) If $P_G^{*(A2)} \neq P_G^{\text{post}}$, add those generators with different dispatch to the set \mathcal{R} , and then go back to 4).
 - 7) Take $P_G^{*(A2)}$ to calculate the cyber power flow of the system.
 - 8) If there exists any cyber overflow, add those lines to \mathcal{Q} , and go back to 4).
 - 9) Let $P_l^{*(A2)}$ be the optimal objective value of the reduced problem.
-

By significantly reducing the number of binary variables, Algorithm 2 can be efficiently applied to the Polish system. Since some of the variables P_G are held constant, the solution is not guaranteed to be optimal for the original MILP. However, it does provide a feasible solution, and hence, $P_l^{*(A2)}$ is a lower bound on P_l^* .

C. Maximizing the Difference between Post-attack Physical and Cyber Power Flows

In this section, we propose Algorithm 3 that provides both lower and upper bounds on P_l^* . In the original MILP the objective is to maximize the physical power flow of a target line, which is calculated by (4). Substituting (4) into (9) gives

$$-P^{\max} - \text{PTDF}(Hc) \leq P \leq P^{\max} - \text{PTDF}(Hc). \quad (22)$$

In particular, for target line l ,

$$P_l \leq P_l^{\max} - \text{PTDF}^l(Hc) \quad (23)$$

TABLE I
COMPARISON OF THREE PROPOSED ALGORITHMS

Algorithm	Type of Program	Outcome	Tractable Test Cases	# of Binary Variables		Computation Time (s)	
				118-bus	Polish	118-bus	Polish
Original MILP	MILP	Optimal Solution	24-bus	480	6446	-	-
Algorithm 1	MILP	Optimal Solution	24-bus, 118-bus	122	688	22.04	-
Algorithm 2	MILP	Lower Bound	24-bus, 118-bus, Polish (2383-bus)	45	87	1.03	40.41
Algorithm 3	LP	Lower & Upper Bounds	24-bus, 118-bus, Polish (2383-bus)	-	-	0.35	4.57

where P_l^{\max} is a constant and PTDF^l is the l^{th} row of the PTDF matrix. Thus, we can maximize $-\text{PTDF}^l(Hc)$ to find an upper bound on P_l^* constrained by (4), (6), and (11). This optimization problem is formulated as

$$\begin{aligned} & \underset{c,s}{\text{maximize}} \quad -\text{PTDF}^l(Hc) \\ & \text{subject to} \quad (4), (6), (11) \end{aligned} \quad (24)$$

This optimization is a linear program and can be solved efficiently for large systems.

Algorithm 3 Maximizing the difference between post-attack physical and cyber power flows

- 1) Solve optimization problem (24). Let c_{A3}^* be the resulting optimal attack vector.
- 2) Calculate the upper bound as

$$P_l^{*(A3,ub)} = P_l^{\max} - \text{PTDF}^l(Hc_{A3}^*). \quad (25)$$

- 3) Perform post-attack DCOFP (7)–(10) with $c = c_{A3}^*$ to find dispatch P_G^{post} .
- 4) Calculate the lower bound as

$$P_l^{*(A3,lb)} = \text{PTDF}^l(G_B P_G^{\text{post}} - P_D). \quad (26)$$

Once the optimal objective is reached, $P_l^{*(A3,ub)}$, can be calculated by adding this optimal objective to P_l^{\max} according to (23). The system re-dispatch P_G^{post} and line cyber power flow P^{cyber} are achieved by performing post-attack DCOFP (7)–(10). The resulting physical power flow on the target line, $P_l^{*(A3,lb)}$, is a lower bound on P_l^* .

Note that if the load shift is too large, it is possible that the post-attack DCOFP fails to converge. However, since we keep the load shift small, this situation is beyond the scope of this paper. Furthermore, if $P_l^{*(A3,ub)} = P_l^{*(A3,lb)}$, they are the optimal objective of the original MILP. This is the situation when $|P_l^{\text{cyber}}| = P_l^{\max}$, *i.e.*, (9) holds with equality in the optimal solution of post-attack DCOFP (7)–(10).

V. SIMULATION RESULTS

In this section, we apply algorithms described in Sec. IV to both the IEEE 118-bus system and the Polish system. As stated in Sec. IV, Algorithm 1 does not converge in reasonable length of time for the Polish system. Therefore, only Algorithms 2 and 3 are applied on the Polish system. There are 7 critical lines prior to the attack in IEEE 118-bus system and 17 in

the Polish system. The number of marginal generators prior to the attack for the two systems are 15 and 6, respectively. We exhaustively evaluate vulnerability of these two systems by targeting all critical lines with load shift constraint $L_S = 10\%$. The l_1 -norm constraint N_1 is chosen as $[0.1, 1]$ for the 118-bus system and $[0.1, 2]$ for the Polish system, both with increment 0.1. GUROBI is utilized as the solver to solve the optimization problem. Throughout, we use MATLAB R2014a and MATPOWER package v4.1 to perform the simulation.

A. Computational Efficiency

The computational efficiency improved by Algorithms 1 and 2 are characterized as the reduction in the number of binary variables. In Table I, the 5th column compares the average numbers of binary variables of the original MILP, Algorithm 1, and Algorithm 2 for both test systems. Note that for the Polish system, the number of binary variables of Algorithms 1 is theoretical, as Algorithm 1 does not converge in a reasonable length of time for the Polish system. The 6th column summarizes the average computation time of the three methods for two typical test cases, *i.e.*, test cases with target line 104 in 118-bus system and target line 292 in the Polish system. As one would expect, Algorithm 3, an LP, is computationally the most efficient among the three proposed algorithms for both test systems.

B. Results for the IEEE 118-bus System

Figs. 1(a) and (b) illustrate the maximum power flow on target lines 104 and 141, respectively, in IEEE 118-bus system using the three different algorithms described in Sec. IV. We use this system to compare the bounds of Algorithms 2 and 3 to the exact solution provided by Algorithm 1; note, however, that the optimal solution of Algorithm 1 is not available for the Polish system. Both figures illustrate that as N_1 increase, P_l^* also increases, and all three algorithms can result in overflow.

Fig. 1(a) shows that for target line with any N_1 , $P_l^{*(A1)} = P_l^{*(A2)} = P_l^{*(A3,ub)} = P_l^{*(A3,lb)} = P_l^*$; that is, all three algorithms achieve the optimal solution of the original MILP. Fig. 1(b) shows that for target line 141, $P_l^{*(A3,lb)} < P_l^{*(A1)} = P_l^{*(A2)} < P_l^{*(A3,ub)}$, illustrating that $P_l^{*(A3,lb)}$ and $P_l^{*(A3,ub)}$ are not always tight bounds on P_l^* . In all scenarios we have considered, Algorithm 2 yields the optimal solution for the 118-bus system. (This is not true for the Polish system, as illustrated in Fig. 2.)

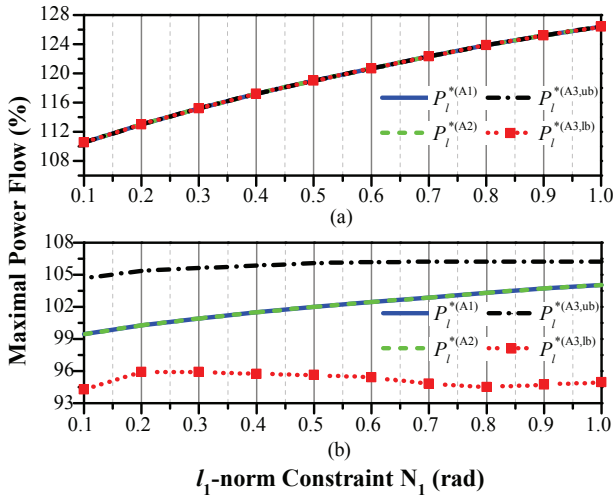


Fig. 1. The maximum power flow v.s. the l_1 -norm constraint (N_1) when target lines are (a) line 104, and (b) line 141 of IEEE 118-bus system.

C. Results for the Polish System

Results for target lines 292, 4, and 1816 obtained with Algorithms 2 and 3 are illustrated in Figs. 2(a), (b), and (c), respectively. We observe that for target line 292, the upper and lower bounds exactly match, *i.e.*, $P_l^{*(A3,ub)} = P_l^{*(A3,lb)} = P_l^{*(A2)}$, in the range $N_1 \in [0.1, 1.6]$, and therefore, the optimal solutions are reached. For the remaining cases, our algorithms do not give the optimal solutions, since $P_l^{*(A3,lb)} < P_l^{*(A2)} < P_l^{*(A3,ub)}$. For target line 4, we observe that the upper and lower bounds do not match, but the lower bound from Algorithm 2 is tighter than that from Algorithm 3, whereas for target line 1816, the opposite is true.

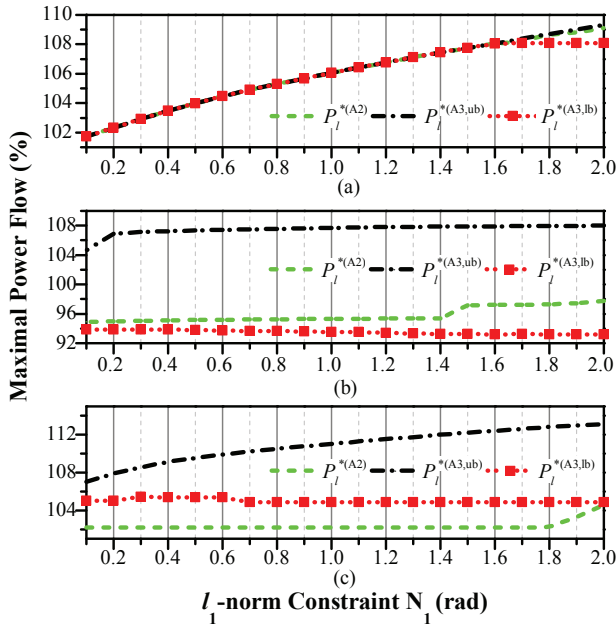


Fig. 2. The maximum power flow v.s. the l_1 -norm constraint (N_1) when target lines are (a) line 292, (b) line 4, and (c) line 1816 of the Polish system.

VI. CONCLUSION

This paper presented an approach to evaluate the vulnerability of power systems to FDI attacks irrespective of the size of the network. Three computationally efficient algorithms have been introduced to characterize the vulnerability of systems. It is demonstrated that Algorithm 1 can find worst-case attacks. Algorithms 2 and 3, on the other hand, can find feasible attacks that can result in significant consequences. Future work will include evaluating attack efficiency for arbitrary system size when attacker only has limited information as in [16] using the three algorithm proposed here. In addition, designing detection countermeasures to thwart such attacks is also of interest.

ACKNOWLEDGMENT

This work is supported jointly by the National Science Foundation and the Department of Homeland Security under Grant CNS-1449080.

REFERENCES

- [1] Y. Liu, P. Ning, and M. K. Reiter, "False data injection attacks against state estimation in electric power grids," in *Proceedings of the 16th ACM Conference on Computer and Communications Security*, ser. CCS '09. New York, NY, USA: ACM, 2009, pp. 21–32.
- [2] O. Kosut, L. Jia, R. J. Thomas, and L. Tong, "Malicious data attacks on the smart grid," *IEEE Transactions on Smart Grid*, vol. 2, no. 4, pp. 645–658, 2011.
- [3] G. Hug and J. A. Giampapa, "Vulnerability assessment of ac state estimation with respect to false data injection cyber-attacks," *IEEE Transactions on Smart Grid*, vol. 3, no. 3, pp. 1362–1370, Sept 2012.
- [4] J. Kim and L. Tong, "On topology attack of a smart grid: Undetectable attacks and countermeasures," *IEEE JSAC*, vol. 31, no. 7, pp. 1294–1305, 2013.
- [5] J. Zhang and L. Sankar, "Physical system consequences of unobservable state-and-topology cyber-physical attacks," *IEEE Transactions on Smart Grid*, vol. PP, no. 99, pp. 1–10, 2016.
- [6] D. Kundur, X. Feng, S. Liu, T. Zourmtos, and K. L. Butler-Purry, "Towards a framework for cyber attack impact analysis of the electric smart grid," in *Smart Grid Communications (SmartGridComm), 2010 First IEEE International Conference on*, Oct 2010, pp. 244–249.
- [7] L. Xie, Y. Mo, and B. Sinopoli, "Integrity data attacks in power market operations," *IEEE Transactions on Smart Grid*, vol. 2, no. 4, pp. 659–666, Dec 2011.
- [8] J. Liang, L. Sankar, and O. Kosut, "Vulnerability analysis and consequences of false data injection attack on power system state estimation," *IEEE Transactions on Power Systems*, vol. PP, no. 99, pp. 1–9, 2016.
- [9] Y. Yuan, Z. Li, and K. Ren, "Modeling load redistribution attacks in power systems," *IEEE Transactions on Smart Grid*, vol. 2, no. 2, pp. 382–390, June 2011.
- [10] —, "Quantitative analysis of load redistribution attacks in power systems," *IEEE Transactions on Parallel and Distributed Systems*, vol. 23, no. 9, pp. 1731–1738, Sept 2012.
- [11] L. Jia, J. Kim, R. J. Thomas, and L. Tong, "Impact of data quality on real-time locational marginal price," *IEEE Transactions on Power Systems*, vol. 29, no. 2, pp. 627–636, March 2014.
- [12] K. Zetter, "Inside the cunning, unprecedented hack of Ukraine's power grid," March 2016. [Online]. Available: <http://www.wired.com/2016/03/inside-cunning-unprecedented-hack-ukraines-power-grid/>
- [13] S. Boyd and L. Vandenberghe, *Convex Optimization*. Cambridge University Press, 2004.
- [14] "California Independent System Operator (CAISO): Technical bulletin 2009-06-05: Market optimization details," June 2009. [Online]. Available: <http://www.caiso.com/23cf/23cfe2c91d880.pdf>
- [15] "Electric Reliability Council of Texas (ERCOT) nodal protocols," January 2015. [Online]. Available: http://ercot.com/mktrules/nprotocols/2015/02/February_2,_2015_Nodal_Protocols.pdf
- [16] J. Zhang, Z. Chu, L. Sankar, and O. Kosut, "False data injection attacks on power system state estimation with limited information," in *IEEE PES General Meeting*, Boston, MA, July 2016.